A Multiphase PWM RF Modulator Using a VCO-Based Opamp in 45nm CMOS

Min Park*, Michael H. Perrott†
*Massachusetts Institute of Technology, Cambridge, MA, USA
(now at Maxim Integrated Products, Sunnyvale, CA, USA)
†SiTime Corporation, Sunnyvale, CA, USA

***Abstract*—A VCO-based RF modulator employing multiphase *Pulse Width Modulation* (PWM) is presented. The proposed RF modulator encodes the baseband signal into a set of multiphase PWM signals which are generated by a VCO-based opamp. The use of PWM avoids broadband quantization noise which is produced by ΣΔ modulation used in other RFDAC-based modulators. The prototype IC is fabricated in a 45nm CMOS process, consumes 54.3 mW, and has an active area of 0.126 mm^2. The measured results satisfy the 802.11g WLAN spectral mask, and EVM for 10-MHz, 64 QAM OFDM at 2.4 GHz is –30 dB.**

***Index Terms*—Pulse width modulation, PWM, Multiphase PWM, RFDAC, RF modulator.**

I. Introduction

Modern CMOS processes have brought many advantages for digital circuits such as high density and high speed. In contrast, analog circuits must deal with reduced supply voltages, higher levels of mismatch, and reduced intrinsic gain. More importantly, these analog circuits are often placed within chips that are largely digital in nature, which creates challenges in achieving a seamless design flow for the overall system. For these reasons, there has been much interest in achieving analog functionality with reduced analog design effort.

In this paper, we examine this goal in the context of achieving an RF modulator structure that avoids the need for CMOS transistors with highly linear transconductance and high intrinsic gain. To do so, full swing signals are utilized whose information is encoded in the form of pulse widths. By using time as the primary signal domain, we take advantage of the steadily improving transition times offered by modern CMOS processes.

Fig. 1 provides an overview of several different methods to achieve a CMOS RF modulator. In each case, we assume that the LO signal is composed of a simple set of switches that are driven with a large-swing signal corresponding to the carrier frequency. However, the data devices can be driven in a variety of ways. In part (a), the data signal consists of a small-signal analog waveform representing the baseband signal, and linear transconductors are required for the data devices. In part (b), the data signal is composed of a full-swing signal that is produced by a ΣΔ modulator with the baseband signal as its input [1], [2]. The impact of ΣΔ modulation is to produce broadband quantization noise which must be kept adequately small to satisfy transmitter spectral mask requirements. The quantization noise can be reduced by the combination of having a high clock rate for the ΣΔ modulator, high frequency

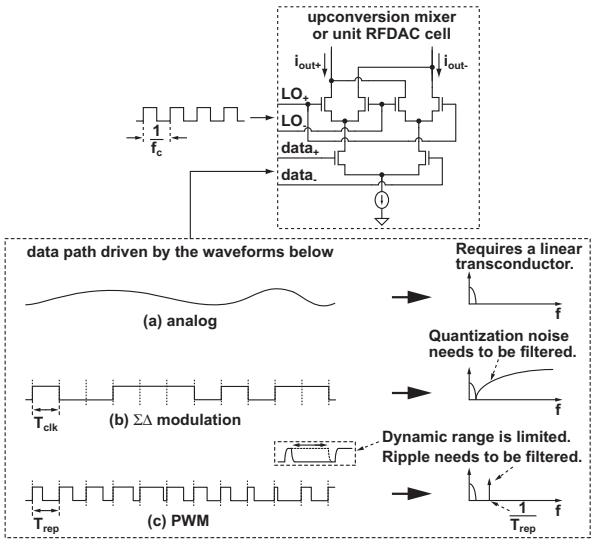

Fig. 1. Various modulation methods for RF upconversion. (a) analog, (b) ΣΔ modulation, (c) PWM.

bandpass filtering of the modulator output [1], [2], or multi-level quantization through the use of several parallel modulator stages with excellent matching [3]. Unfortunately, utilization of bandpass filtering or multi-level modulation brings non-trivial analog design challenges, and simply using a high clock rate for the ΣΔ modulator will often prove inadequate to achieve spectral mask requirements of the modulator.

Part (c) of Fig. 1 shows the use of PWM to achieve a full-swing signal for the data path [4]. Unlike ΣΔ modulation which maintains a constant time period for data samples, PWM allows continuous adjustment of its pulse width in analog fashion. As such, the broadband quantization noise of ΣΔ modulation is avoided and replaced with ripple whose primary frequency content occurs at the pulse repetition frequency. A key goal is to place the pulse repetition frequency high enough in value to be easily filtered at the modulator output. However, due to finite transition times of the PWM edges, a high pulse repetition frequency also leads to reduced dynamic range [5].

As shown in Fig. 2, multiphase PWM improves the tradeoff between achieving high frequency ripple and wide dynamic range. By adding PWM signals that are offset in time with each other, the resulting *effective* ripple frequency is dramatically increased compared to the base pulse repetition rate of the individual signals [6], [7]. The addition of such multiphase

978-1-4244-6241-4/978-1-4244-6242-1/
978-1-4244-6243-8/10/$26.00 © 2010 IEEE

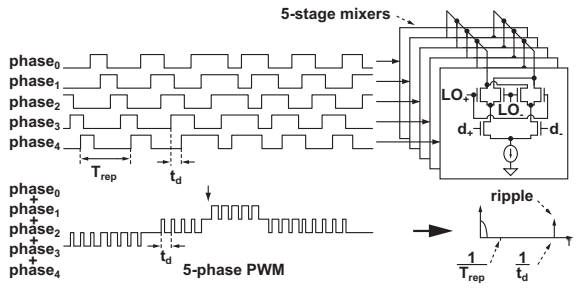

Fig. 2. The waveforms and spectrum of multiphase PWM signals.

PWM signals is achieved by using several mixer stages in parallel. While a $\Sigma\Delta$-based mixer could also utilize parallel stages to achieve a multi-level implementation, any mismatch between stages can lead to noise folding and spur generation in the modulator output. In contrast, when using the multiphase PWM approach, mismatch between stages simply leads to increased leakage of the base pulse repetition frequency (which is relatively high in frequency) to the modulator output.

The use of multiphase PWM is not a new concept, but previous approaches have involved fairly analog intensive circuit structures. As an example, the approach presented in [8] employs triangular waveform generators and multilevel comparators. In this paper, we propose the use of a relatively simple VCO-based opamp to achieve multiphase PWM which offers several implementation advantages in modern CMOS technology. Using this VCO-based opamp, we demonstrate a multiphase PWM modulator that satisfies the 802.11g WLAN spectral mask.

II. VCO-BASED OPAMP

To explain the concept of a VCO-based opamp, we begin by illustrating a unity gain amplifier that is achieved with two voltage-controlled ring oscillators, a set of XOR phase detectors and current DACs, and a simple RC filter as shown in Fig. 3. The two VCOs act as integrators from input voltage to output phase, and the XOR phase detectors and current DACs convert the phase difference between the two VCO outputs into an overall current signal which is then filtered to form the output voltage. One VCO tuning input is controlled by the input voltage, V_{in}, and the other VCO tuning input is controlled through feedback from the output voltage. While the phase detection operation of the VCO opamp has ripple that must be filtered out, the frequency of the ripple is quite high due to the multiphase principle discussed earlier in this text. As such, the ripple can be substantially attenuated with a low area RC filter.

In effect, the VCO-based opamp is a phase-locked loop (PLL) that maintains the same frequency for each VCO. As the input tuning voltage of one of the VCOs is altered according to the input, the other VCO tuning voltage tracks the input by virtue of feedback. Assuming perfect matching between the VCOs, a perfect match in input and output voltages is achieved since phase-locking forces equal VCO frequencies. Also, since the feedback signal is formed as the average of the

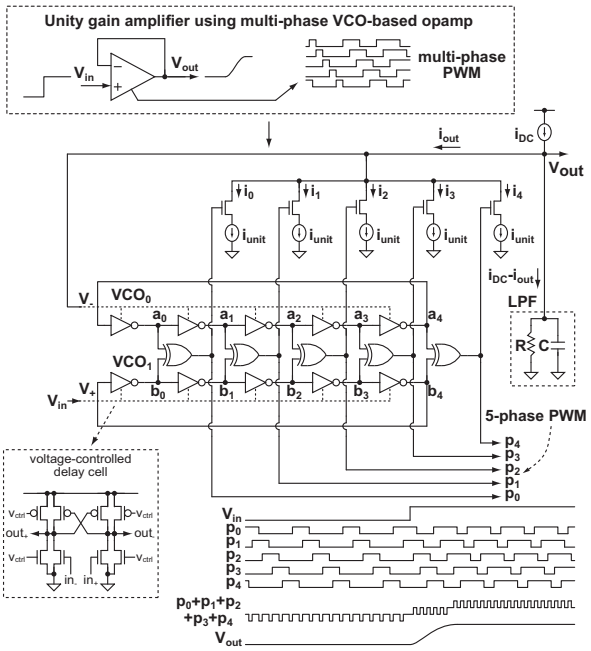

Fig. 3. A unity gain amplifier using a multiphase VCO-based opamp.

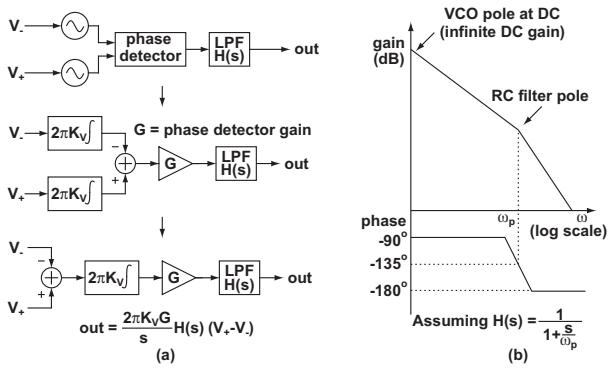

Fig. 4. (a) VCO-based opamp and its model. (b) The open loop Bode plot of a VCO-based opamp when the LPF is a simple RC filter.

multiphase PWM signals, the duty cycle of those multiphase PWM signals also track the input. As such, the VCO-based opamp is seen as an elegant structure for generating multiphase PWM signals. The pulse repetition rate of the individual PWM signals is set by the VCO frequency as controlled by the input. The effective ripple of the addition of the multiphase PWM signals is $\frac{1}{t_d}$, where t_d is set by the delay element used in the ring VCOs. Since a delay of a few tens of picoseconds can be easily achieved in modern CMOS processes, the effective ripple frequency of the VCO-based opamp can be set on the order of tens of GHz. As mentioned earlier, a simple RC filter is sufficient to suppress such ripple.

To better understand the VCO-based opamp, a simplified model is shown in Fig. 4 along with its associated open loop Bode plot. As shown by the model, the VCO-based opamp effectively integrates the difference in input voltages. The Bode plot in Fig. 4 reveals a fairly simple open loop response

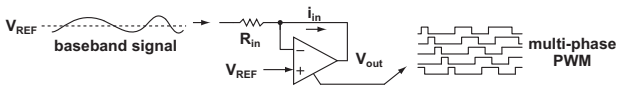

Fig. 5. Multiphase PWM generation using a VCO-based opamp.

consisting of the integrator and RC filter pole. To achieve robust, stable operation, the unity gain crossover frequency should be set less than the value of the RC filter pole.

A very interesting advantage of the VCO-based opamp is that it has infinite DC gain in its open loop transfer function due to the voltage-to-phase integration operation of the VCO circuits. In contrast, traditional opamp structures must resort to fairly complicated techniques such as nested Miller topologies [9] to achieve both high open loop DC gain and proper compensation since the intrinsic gain of devices is steadily degrading in modern CMOS processes.

However, there are, of course, disadvantages to the proposed VCO-based opamp structure. One key issue is that there is a limited locking range offered by the phase detectors within the VCO-based opamp, and one needs to worry about avoiding cycle slips during steady-state operation as encountered with other PLL circuits. The limited locking range imposes constraints on the allowable voltage and frequency variation at the input [10]. Another issue is that a practical ring VCO has a nonlinear tuning characteristic for its gain, K_V. This nonlinearity can lead to distortion at the output of the unity-gain VCO-based opamp when the input is varied at high frequencies. More importantly, large changes in K_V can lead to stability problems since the unity gain crossing frequency of the VCO-based opamp is a direct function of K_V.

III. Proposed RF modulator employing a VCO-based Opamp

When utilizing the VCO-based opamp for a multiphase PWM modulator, it is advantageous to use the unity-gain amplifier configuration shown in Fig. 5. In this case, the input of the amplifier is set by a reference voltage V_{REF} that can be chosen for optimal performance of the modulator (such as setting an appropriate PWM repetition rate or achieving a desired nominal K_V value). A key advantage offered by this constant input voltage is that variation in the nominal K_V value is greatly reduced so that stable operation is easily achieved, and the PWM repetition frequency is fairly constrained.

Due to the feedback action of the opamp, the output voltage is also held at V_{REF}. However, if we inject current into the output, the pulse widths of the PWM signals generated by the VCO-based opamp must appropriately adjust their value in order to maintain the output voltage at V_{REF}. Therefore, we can easily create an input voltage to multiphase PWM generator by simply connecting a resistor between the baseband voltage signal and VCO-based opamp output.

While the proposed VCO-based multiphase PWM generator shown in Fig. 5 alleviates large variations in nominal K_V, the nonlinearity of the VCO K_V characteristic limits distortion

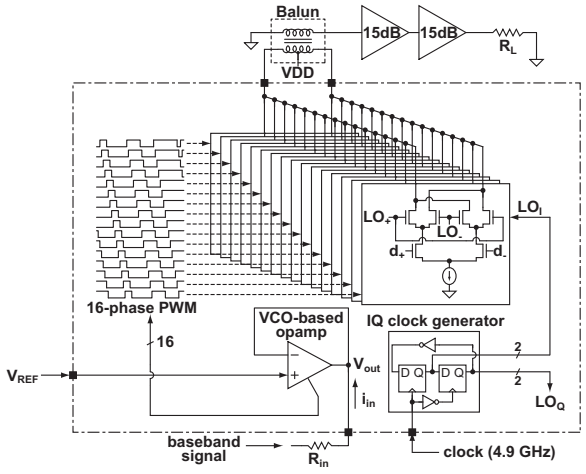

Fig. 6. Simplified block diagrams of the proposed VCO-based RF modulator chip. Only the in-phase signal path is shown for simplicity.

performance for large amplitude, high frequency input signals. To explain, the negative feedback loop of the multiphase PWM generator suppresses the VCO nonlinearity by keeping the VCO tuning voltage constant when the input signal is slowly varying. However, the feedback loop cannot instantaneously track a large amplitude, fast-varying input signal variation. The frequency dependency of nonlinearity suppression is a key design consideration for wideband modulation as pursued in this paper. As will be shown by measured results later in this paper, its impact can be reasonably mitigated for moderate performance applications such as WLAN.

The overall architecture of the proposed RF modulator is shown in Fig. 6. Both I and Q channels are included in the actual chip, but Fig. 6 shows only the I channel signal path for simplicity. Most of the signal paths are differential except for the baseband signal path. The digital blocks employ full-swing pseudo differential logic.

16-stage mixer cells are employed in the prototype chip. The 16-phase PWM signals generated from the VCO-based opamps drive the 16 mixer cells to create the desired RF signal. One advantage of this architecture is that the ring VCOs and phase detectors sequentially drive the current DACs and mixer cells, such that *Dynamic Element Matching* (DEM) is achieved for free. A similar DEM effect in a VCO-based A/D converter is reported in [11]. Accordingly, the matching requirement for the mixer cells and current DACs is reasonably relaxed.

An on-chip frequency divider generates the IQ LO clocks. Note that IQ mismatch occurs due to non-idealities of the frequency divider such as duty cycle and delay mismatch [12], and due to gain/phase mismatch of the VCO-based opamps for the IQ channels. Compensation of this IQ mismatch is achieved in the prototype by manual gain and phase predistortion in an off-chip baseband signal generator.

IV. Measured results

The proposed VCO-based RF modulator is implemented in a 45nm CMOS process with an active area of 0.126 mm^2. The

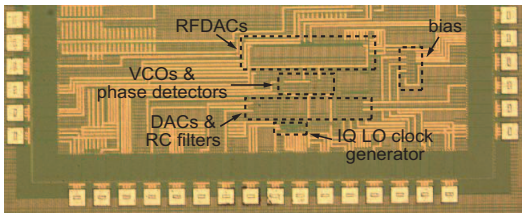

Fig. 7. Die photograph of the implemented VCO-based RF modulator.

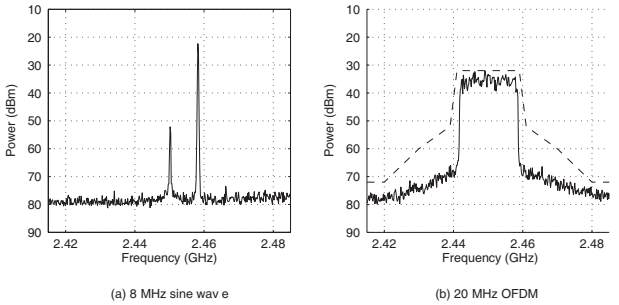

Fig. 8. (a) Measured output spectrum with a 8-MHz sine wave, (b) Measured 20-MHz OFDM output spectrum compared to 802.11g spectral mask.

die photograph is shown in Fig. 7. Total power consumption of the chip is 54.3 mW including LO clock buffer, mixers, bias, VCOs and other digital circuits. The IQ baseband signals are generated by an arbitrary function generator. The output signal from the chip is amplified by two 15-dB amplifiers before the signal is measured by a spectrum analyzer.

Fig. 8 (a) shows the modulator's in-band output spectrum at 2.45 GHz when the input signal is an 8-MHz sine wave. IQ mismatch compensation is done manually on the input baseband IQ signals in order to suppress image signals. Fig. 8 (b) shows the 20-MHz OFDM output spectrum centered at 2.45 GHz. The spectrum is compared with an 802.11g spectral mask as a reference.

For the EVM test, a 10-MHz, 64 QAM OFDM signal for 802.11a WLAN is used as a baseband signal. 10-MHz of bandwidth is chosen since the test equipment is limited to this value. The generated source signals are predistorted for IQ mismatch compensation in a PC. The predistorted baseband signals are loaded into a vector signal generator, which sends the baseband IQ signals to the chip. The measured EVM with IQ mismatch compensation is about –30 dB, as is shown in the fourth quadrant of Fig. 9. The plot in the first quadrant of Fig. 9 shows the EVM at each frequency bin and reveals that the highest EVM values occur close to the carrier frequency, which is likely due to upconverted flicker noise of the VCOs. The more detailed measurement results can be found in [10].

V. Conclusion

A multiphase PWM RF modulator in 45nm CMOS technology was presented which achieves upconversion of a baseband signal by using multiphase PWM signals generated by a VCO-based opamp. The prototype chip demonstrates that the proposed RF modulator is capable of upconverting a 20-MHz,

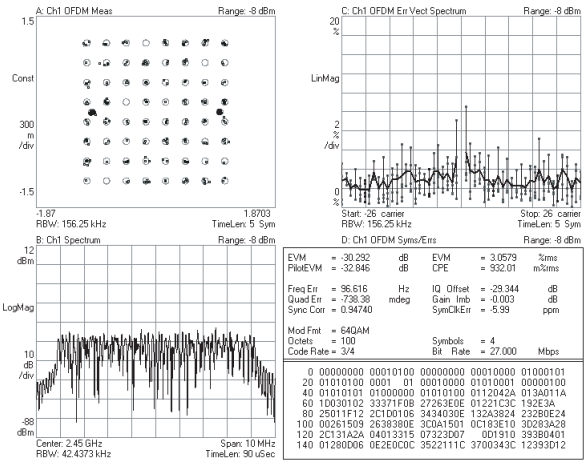

Fig. 9. Measured EVM with a 10-MHz OFDM signal for 802.11a WLAN.

64 QAM OFDM signal at 2.4 GHz while meeting 802.11g output spectral mask requirements.

Acknowledgment

Texas Instruments Inc. provided chip fabrication. The authors would like to thank Dennis Buss, Alice Wang, and Chih-Ming Hung, Texas Instruments Inc. for their support.

References

[1] A. Jerng and C. G. Sodini, "A wideband $\Delta\Sigma$ digital-RF modulator for high data rate transmitters," *IEEE J. Solid-State Circuits*, vol. 42, no. 8, pp. 1710–1722, Aug. 2007.

[2] S. M. Taleie, Y. Han, T. Copani, B. Bakkaloglu, and S. Kiaei, "A 0.18μm CMOS fully integrated RFDAC and VGA for WCDMA transmitters," *Proc. IEEE RFIC Symposium*, pp. 157–160, June 2008.

[3] P. Eloranta, P. Seppinen, S. Kallioinen, T. Saarela, and A. Pärssinen, "A multimode transmitter in 0.13μm CMOS using direct-digital RF modulator," *IEEE J. Solid-State Circuits*, vol. 42, no. 12, pp. 2774–2784, Dec. 2007.

[4] J. S. Walling, H. Lakdawala, Y. Palaskas, A. Ravi, O. Degani, K. Soumyanath, and D. J. Allstot, "A class-E PA with pulse-width and pulse-position modulation in 65nm CMOS," *IEEE J. Solid-State Circuits*, vol. 44, no. 6, pp. 1668–1678, June 2009.

[5] S. Kuo, "Linearization of a pulse width modulated power amplifier," *S.M. Thesis*, Massachusetts Institute of Technology, 2004.

[6] S. Abedinpour, B. Bakkaloglu, and S. Kiaei, "A multistage interleaved synchronous buck converter with integrated output filter in 0.18μm SiGe Process," *IEEE Trans. Power Electron.*, vol. 22, no. 6, pp. 2164–2175, Nov. 2007.

[7] T. Carosa, R. Zane, and D. Maksimović, "Scalable digital multiphase modulator," *IEEE Trans. Power Electron.*, vol. 23, no. 4, pp. 2201–2205, July 2008.

[8] B. A. Weaver, "A new, high efficiency, digital, modulation technique for AM or SSB sound broadcasting application," *IEEE Trans. Broadcasting*, vol. 38, issue 1, pp. 38–42, March 1992.

[9] J. H. Huijsing and D. Linebarger, "Low-voltage operational amplifier with rail-to-rail input and output ranges," *IEEE J. Solid-State Circuits*, vol. SC-20, no. 6, pp. 1144–1150, Dec. 1985.

[10] M. Park, "Time-based circuits for communication systems in advanced CMOS technology," *Ph.D. Thesis*, Massachusetts Institute of Technology, 2009.

[11] M. Z. Straayer and M. H. Perrott, "A 10-bit 20MHz 38mW 950MHz CT $\Sigma\Delta$ ADC with a 5-bit noise-shaping VCO-based quantizer and DEM circuit in 0.13μm CMOS," *Proc. IEEE Symposium on VLSI Circuits*, pp. 246–247, June 2007.

[12] C. D. Renter and M. Steyaert, *High data rate transmitter circuits: RF CMOS design and techniques for design automation*, Kluwer Academic Publishers, 2003.